

Geometry of Thin Films

Ron Perline, Department of Mathematics
Drexel University, Philadelphia, PA 19104
email: ronald.k.perline@drexel.edu

(Submitted to the Journal of Nonlinear Science, 9.17.2015)

Abstract

We study ray optics in the context of double mirror systems, in the limit as the two mirrors approach one another (thin films). This leads to a novel set of differential equations on a mirror surface which have interesting structure as seen from the perspective of symplectic geometry and Hamiltonian mechanics.

1 Introduction

In optics, the phrase "thin films" refers to optical materials for which one dimension is so much smaller than the other two that it affects the physics of light transmission in the film medium. For technological reasons (the difficulty of actually producing such films), the subject was not investigated until the early 1920's (see [1] for a historical background prior to the 1960's). By now, there is an enormous literature devoted to the physical properties of such films, optical and otherwise (for a recent summary, see [2]). In the design of such thin films, one can consider inhomogeneities in the film material itself; or the film can be constructed from a homogeneous material, but with varying thickness. Many experimental studies of the latter case have been conducted, going back as far as the early 70's ([3], [4]).

Depending on the thickness of the film, light transmission can be modelled using the ray optics approximation, with the light rays "bouncing" from top to bottom; these two surfaces acting like nearby reflecting surfaces (mirrors).

Our interest in optics of thin films was stimulated by a question posed by S. Tabachnikov regarding the relationship between symplectic geometry and mirrors. We present his problem using the language of symplectic geometry and hamiltonian mechanics, and show the connection to ray optics in thin films. These considerations will lead to a novel set of differential equations associated with a surface embedded in R^3 , or more generally, hypersurfaces. For appropriate choice of parameters, one can obtain billiard dynamics and geodesic flow as special cases of these equations.

Consider $V = R^n \oplus R^n$, endowed with the standard inner product. Via this inner product, we can identify T^*S^N , the cotangent bundle of the sphere, with its tangent bundle, and with the set

$$G_1 = \{(x, y) \in V \mid \langle x, x \rangle = 1, \langle x, y \rangle = 0\}$$

We can use G_1 to parameterize \mathcal{G} , the Grassmannian of oriented lines in R^n , in the following manner: given an oriented line $\mathbf{l} \in \mathcal{G}$, we associate to it its unit direction vector $x = x(\mathbf{l})$, and the unique vector along \mathbf{l} , $y = y(\mathbf{l})$, such that $\langle x, y \rangle = 0$.

As a result of this identification, \mathcal{G} inherits a symplectic structure from T^*S^{n-1} . We mention a few references which can be useful here: for general information about symplectic geometry, see [5]; for specific information about the geometry of \mathcal{G} , see [6]; a discussion of the symplectic geometric approach to a related topic, *thin lens* theory, can be found in [7].

Given a surface M , it induces (via reflection) a mapping on \mathcal{G} , and it is known that this is a symplectic map. Clearly, not all symplectic maps can be realized in this manner, which leads to a question of Tabachnikov's: which ones are? One can obviously expand the question to

include multi-mirror systems, in particular pairs of mirrors, and this is the particular case we will address: what are the symplectic maps on \mathcal{G} induced by double mirror systems.

At the moment, we cannot answer this question. However, we can make progress on a simpler, “infinitesimal” version of it. To explain this, we need a few definitions.

Given an orientable surface M_0 , let Φ_{M_0} be the associated symplectic map on \mathcal{G} . We consider surfaces nearby M_0 as graphs in the normal bundle of M_0 ; let $f : M_0 \rightarrow \mathbb{R}$ (we will refer to f as the *displacement function*) and use this to construct a one-parameter family of surfaces $M_\epsilon = \{p + \epsilon f(p)N(p), p \in M_0\}$, where $N(p)$ denotes the unit normal. With $\Phi \equiv \Phi_{M_0}$, and $\tilde{\Phi} \equiv \Phi_{M_\epsilon}$, we consider the composition $\Phi^{-1}\tilde{\Phi}$, corresponding to the double mirror system consisting of M_0 and M_ϵ . Note that, for any mirror M , Φ_M is an involution.

For ϵ small, this composition should be close to the identity map, and in fact one expects (since $\Phi^{-1}\tilde{\Phi}$ is symplectic) that $\chi_f = \frac{d}{d\epsilon}(\Phi^{-1}\tilde{\Phi})|_{\epsilon=0}$ should be a hamiltonian vector field on \mathcal{G} , with some Hamiltonian H_f . So the infinitesimal version of Tabachnikov’s question for double mirror systems is: what distinguishes the Hamiltonians H_f among general Hamiltonians on \mathcal{G} ? Note: we write “hamiltonian” if the word is being used as an adjective, and “Hamiltonian” if it is being used as a noun. For obvious reasons, we will refer to these systems which are limiting versions of double mirror systems as *thin films*.

To most easily express a formula for H_f , we need a different parameterization of \mathcal{G} which is better suited to our context. Suppose we have a surface M ; given an oriented line $\mathbf{l} \in \mathcal{G}$, we consider (as before) the unit direction vector $v = v(\mathbf{l})$, as well as “the” intersection point $p = p(\mathbf{l})$ of \mathbf{l} with the surface M (the existence and uniqueness of p depends of course on the geometry of M and relative positioning of v). In other words, we are parameterizing \mathcal{G} by the set $G_2 = S^{n-1} \times M \subset V$. We have the map $T : G_2 \rightarrow G_1$ defined by $(v, p) \rightarrow (v, p - \langle p, v \rangle v)$, which allows one to pull back the symplectic structure from G_1 to G_2 . We will freely identify points in G_2 with corresponding points in \mathcal{G} .

The vector field χ_f can, via the above identifications, be considered as a vector field on G_2 . Then χ_f corresponds to the Hamiltonian

$$H_f(v, p) = -2\langle v, N(p) \rangle f(p) \ .$$

The formula for χ_f is given by Eqn. (1) of the next section.

Naturally, this raises the following question: for a given H on \mathcal{G} , how do we know there exists an M and f so that $H = H_f$? This question is not yet solved; however, it is likely that there is some differential condition which needs to be satisfied. Notice, for example, in the form given above, that the differential of H_f with respect to the v variable is independent of v .

The structure of this paper is as follows: In Section 2, we explicitly obtain the formula for χ_f on G_2 . In Section 3, we show that the Hamiltonian indicated above does indeed correspond to χ_f . In Section 4, we discuss the dynamical interpretation of χ_f and its relation to multiple reflections. Sections 5 and 6 show connections between this dynamical problem, geodesic flow, and billiard dynamics. Section 7 gives another formulation of our equations coming from a related variational problem, which can be more convenient to work with. We then give a fairly complete discussion to one concrete problem: the dynamical problem associated with a spherical displacement function. This is followed by a brief discussion of the dynamical problem associated with an ellipsoidal displacement function. Section 8 considers “error estimates” comparing the dynamical problem associated with χ_f and the discrete system of multiple reflections inside the thin film. Section 9 describes some bracket relations for the types of Hamiltonians we are considering: it indicates that there is a natural

Lie algebra (generated by the Hamiltonians H_f) which includes a subalgebra isomorphic to the vector fields on the mirror surface (with the standard Lie bracket). Section 10 contains some concluding remarks.

The goal of this paper is to introduce χ_f and its various basic properties. We briefly make some comments about some cases where the associated dynamical problem is integrable; a fuller treatment of more extensive integrable cases will be treated in a subsequent publication.

2 Computation of χ_f on G_2

The procedure for the explicit computation of χ_f is graphically indicated in Figure 1. We give a brief summary of the steps involved. First a remark: we will need to compute the objects and quantities mentioned below modulo terms of order ϵ^2 , and we will write $A \simeq B$ if $A - B = O(\epsilon^2)$. In the following, “compute” will mean “compute modulo terms of order 2 or higher in ϵ ”. Hopefully, this will not cause confusion.

Let’s fix ϵ small, and denote $M = M_0$, $\tilde{M} = M_\epsilon$; $\Phi, \tilde{\Phi}$ are as before. We have discussed the map Φ , but have not yet described it explicitly. Let \mathfrak{l} be a line in \mathcal{G} represented by a point $(v, p) \in G_2$, then $\Phi(v, p) = (v_r, p)$, where $v_r = v - 2\langle v, N(p) \rangle N(p)$. “Above” each point $p \in M$ is a corresponding point $\tilde{p} = p + \epsilon f(p)N(p)$ (f could of course be negative). At \tilde{p} there is $\tilde{N}(\tilde{p})$ which is normal to \tilde{M} . We will need to compute \tilde{N} in terms of M and f .

To compute $\tilde{\Phi}$ applied to a line \mathfrak{l} , we will need the point of intersection of \mathfrak{l} with \tilde{M} , which we call \tilde{i} , as well as the normal $\tilde{N}(\tilde{i})$ at that point. $\tilde{i} = i + \epsilon f(i)N(i)$ for some point i on M ; knowing i will allow us to compute $\tilde{N}(\tilde{i})$. With this information, we can compute $\tilde{v}_r = v - 2\langle v, \tilde{N}(\tilde{i}) \rangle \tilde{N}(\tilde{i})$.

To complete the evaluation of $\tilde{\Phi}(\mathfrak{l})$, we need to find the point of intersection q of the reflected line with the surface M .

Finally, our goal is to compute $\Phi^{-1}\tilde{\Phi}(\mathfrak{l})$. To do so, we will need to reflect \tilde{v}_r at the point q ; $w = \tilde{v}_r - 2\langle \tilde{v}_r, N(q) \rangle N(q)$. Thus, $\Phi^{-1}\tilde{\Phi}(\mathfrak{l})$ has coordinate representation $(w, q) = (w(\epsilon), q(\epsilon))$ in G_2 . We emphasize: all the quantities and terms described above are computed modulo ϵ^2 . At this point, we will compute $\frac{d}{d\epsilon}(w, q)|_{\epsilon=0}$, giving us the desired vectorfield χ_f on G_2 .

Although elementary, the calculation is somewhat tedious; the details will appear in the published version of this paper. After these calculations, one obtains:

The variation vector field $\chi_f(v, p)$ on G_2 is given by

$$-2 (\langle v, -uW + \nabla f \rangle N - \langle v, N \rangle (-uW + \nabla f), -u\pi(v)), \quad (1)$$

where the dependencies $W = W(\pi(v))$, $f = f(p)$, $N = N(p)$ are suppressed for readability, and $u = \frac{f(p)}{\langle v, N(p) \rangle}$ as before; W denotes the Weingarten map for the surface M .

3 The Symplectic Structure and the Hamiltonian

In addition to an inner product, $V = R^n \oplus R$ has a symplectic structure: if $w_1 = (v_1, p_1)$, $w_2 = (v_2, p_2) \in V$, then $\Omega_1(w_1, w_2) = \langle v_1, p_2 \rangle - \langle v_2, p_1 \rangle$. As a result of a simple calculation (or obviousness) the symplectic structure on G_1 that one obtains via the identification of G_1 with T^*S^{n-1} is just the restriction of Ω_1 to G_1 . Let’s now discuss the symplectic structure on G_2 . In the introduction, we defined a map $T : G_2 \rightarrow G_1$, which can be extended to a mapping from V to V . We can use this to pull back the symplectic structure on G_1 to G_2 . This is the same considering T as a map from V to V , computing the pullback of Ω_1 via T (call this Ω_2) and then restricting Ω_2 to G_2 . $\Omega_1 \neq \Omega_2$ on V , but the two forms are equal

when restricted to G_2 . Let's show this. From the definition of T , considered as a map on V one computes that

$$dT(\Delta v, \Delta p) = (\Delta v, \Delta p - \langle \Delta p, v \rangle v - \langle p, \Delta v \rangle v - \langle p, v \rangle \Delta v) .$$

This can be conveniently written in matrix form:

$$\begin{bmatrix} I_n & 0_n \\ (p^\dagger v) I_n - vp^\dagger & I_n - vv^\dagger \end{bmatrix} \begin{bmatrix} \Delta v \\ \Delta p \end{bmatrix} .$$

Abusing notation, we will refer to this $2n \times 2n$ matrix as dT . Ω_1 can be represented by the matrix J , with

$$J = \begin{bmatrix} 0_n & I_n \\ -I_n & 0_n \end{bmatrix} ,$$

and so the matrix representation of $\Omega_2 = dT^\dagger J dT$ is

$$J_2 = \begin{bmatrix} pv^\dagger - vp^\dagger & I_n - vv^\dagger \\ -I_n + vv^\dagger & 0_n \end{bmatrix} .$$

Of course, by this we mean the following: if $w_i = (\Delta v_i, \Delta p_i)$, $i = 1, 2$ then $\Omega_2(w_1, w_2) = w_1^\dagger J_2 w_2$. Let us now restrict our attention to vectors tangent to G_2 , which means we are considering Δv_i and Δp_i with $\langle \Delta v_i, v \rangle = 0$ and $\langle \Delta p_i, N(p) \rangle = 0$. Under these conditions, we have $w_1^\dagger J_2 w_2 = w_1^\dagger J w_2$.

Using J , we can compute the co-vector associated to the vector $\tilde{\chi}_f = \frac{-\chi_f}{2}$; application of this co-vector to a vector is just the result of the matrix multiplication

$$\begin{bmatrix} (\Delta v)^\dagger & (\Delta p)^\dagger \end{bmatrix} \begin{bmatrix} -u\pi(v) \\ -\langle v, -uW + \nabla f \rangle N + \langle v, N \rangle (-uW + \nabla f) \end{bmatrix} .$$

Let's look at the term involving Δv . We obtain:

$$\begin{aligned} A = \langle \Delta v, -u\pi(v) \rangle &= -u \langle \Delta v, v - \langle v, N \rangle N \rangle \\ &= -u \langle \Delta v, -\langle v, N \rangle N \rangle \\ &= u \langle v, N \rangle \langle \Delta v, N \rangle \\ &= \langle \Delta v, N \rangle f(p) . \end{aligned}$$

Treating the terms which include Δp , we have

$$\begin{aligned} B &= \langle \Delta p, -\langle v, -uW + \nabla f \rangle N + \langle v, N \rangle (-uW + \nabla f) \rangle \\ &= \langle \Delta p, \langle v, N \rangle (-uW + \nabla f) \rangle \\ &= -u \langle v, N \rangle \langle \Delta p, W \rangle + \langle \Delta p, \nabla f \rangle \langle v, N \rangle \\ &= \langle \Delta p, -W \rangle f(p) + \langle \Delta p, \nabla f \rangle \langle v, N \rangle . \end{aligned}$$

Now, consider the Hamiltonian $\tilde{H}_f(v, p) = \langle v, N(p) \rangle f(p)$. We calculate its differential:

$$\begin{aligned} d\tilde{H}_f(\Delta v, \Delta p) &= \langle \Delta v, N \rangle f(p) + \langle v, -W(\Delta p) \rangle f(p) + \langle v, N \rangle \langle \nabla f, \Delta p \rangle \\ &= \langle \Delta v, N \rangle f(p) + \langle \pi(v), -W(\Delta p) \rangle f(p) + \langle v, N \rangle \langle \nabla f, \Delta p \rangle \\ &= \langle \Delta v, N \rangle f(p) + \langle -W(\pi(v)), \Delta p \rangle f(p) + \langle v, N \rangle \langle \nabla f, \Delta p \rangle \\ &= A + B , \end{aligned}$$

which allows us to conclude that χ_f is indeed the hamiltonian vector field associated with H_f .

4 Dynamical Interpretation of χ_f

The calculations of the previous sections are related to the evaluation of $\frac{d}{d\epsilon}\Phi^{-1}\tilde{\Phi}|_{\epsilon=0}$. Our calculation of χ_f essentially says the following: Start at a point (v_0, p_0) , reflect off \tilde{M} , intersect M at a point p_1 , then reflect again at p_1 . Call the new point in G_2 (v_1, p_1) . Then $(v_1, p_1) \simeq (v_0, p_0) + \epsilon\chi_f(p_0)$.

One can obviously iterate this process, to obtain subsequent points (v_i, p_i) , $i = 0, 1, 2, 3, \dots$. Thus, given a fixed time T_0 , it seems that the time T_0 map of the flow associated to the equation $\frac{dg}{dt} = \chi_f(g)$ on G_2 is the formal limit of the "double reflections" shown in figure 2, iterated $\frac{T_0}{\epsilon}$ times, with spacing between surfaces of order ϵ . To prove this, one can reason along the lines of numerical analysis, where there are "local truncation errors" and "global errors" associated with numerical schemes for solving ODE's (see section 10).

Given this dynamical interpretation, we will refer to the differential equation defined on G_2 given by $\dot{\gamma}(v, p, t) = \chi_f$ (here, " $\dot{\gamma}$ " denotes differentiation with respect to t) as the "Thin Film Equation" (TFE). In the next two sections, we consider two simplified cases: one, where M is an arbitrary (in particular, curved) surface in R^{N+1} and the displacement function is constant; and the second is where the surface M is a plane, and f is an arbitrary displacement function.

For the most part, we will be concentrating on $N = 2$ (M is a surface in 3-space). A note on terminology: the vector v , since it has a normal component, is in general not in the same direction as the tangent vector to the p trajectory; so let's call it the pseudo-velocity.

5 Relation to Geodesic Flow

The situation where M is not planar, and the film is uniform ($f \equiv c$) is interesting; here $H(v, p) = c\langle v, N(p) \rangle$. As we shall now show, the associated film equations are essentially a scaled version of geodesic flow.

In the case $f = c$, the ∇f terms in χ_f disappear, and we are left with

$$u (\langle v, W(\pi(v)) \rangle N(p) - \langle v, N(p) \rangle W(\pi(v)) , \pi(v))$$

Note that ignoring the factor u (which is essentially the reciprocal of the Hamiltonian!) simply causes a change of time scale for the solution to the differential equation, and we will therefore discard it. We have thus arrived at the differential equation system on G_2 ,

$$\frac{dv}{dt} = \langle v, W \rangle N - \langle v, N \rangle W, \quad \frac{dp}{dt} = \pi, \quad (2)$$

where for the moment we use the following abbreviated notation: $W \equiv W(\pi(v))$, $N \equiv N(p)$, $\pi \equiv \pi(v)$, $v_{\perp} \equiv \langle v, N \rangle N$. Note that $\alpha \equiv \langle v, N \rangle$ can be treated as a constant. Thus we have:

$$v = \pi + v_{\perp},$$

$$\frac{dv}{dt} = \langle \pi, W \rangle N - \alpha W,$$

$$\frac{dv}{dt} = \frac{d\pi}{dt} + \frac{dv_{\perp}}{dt}.$$

Now since $v_{\perp} = \alpha N$, we have

$$\frac{dv_{\perp}}{dt} = \alpha \frac{dN}{dt} = -\alpha W.$$

Using this last fact, and the two equations given above involving $\frac{dv}{dt}$, we obtain

$$\frac{d\pi}{dt} = \langle \pi, W \rangle N, \quad \frac{dp}{dt} = \pi$$

One sees easily that $\langle \pi, \pi \rangle$, is constant, so we can rescale t to arclength s so that $\frac{dp}{ds} = T$, where T is the tangent indicatrix. The equations then become

$$\frac{dT}{ds} = \langle T, W(T) \rangle N, \quad \frac{dp}{ds} = T$$

which are the equations for a geodesic on a (hyper)-surface. Thus, our equations (with general f) generalize the notion of light rays on a surface.

6 Flat Substrate Films and Billiards

Consider the situation where M is the plane (so $W = 0$), and $f = f(p) = f(p_1, p_2)$ is some arbitrary function. Then, from the last section, we can visualize the dynamics of the TFE as a “smoothed out” version of the discrete system obtained by a particle (or light ray) bouncing up and down between a flat plate substrate and a nearby, nearly flat contour. Then of course, the differential equation associated with f looks like (we ignore the factor of -2 and rescale by a factor of $\langle v, N \rangle$, which is *not* the Hamiltonian here)

$$\frac{dv}{dt} = \langle v, N \rangle \langle v, \nabla f \rangle N - \langle v, N \rangle^2 \nabla f, \quad \frac{dp}{dt} = -f(p) \pi(v). \quad (3)$$

To get a feel for some of the possible dynamics, consider the plots in Figures 3-6. The caption for each plot gives the displacement function f , and the initial values of v and p respectively (for these plots, p_1 and p_2 refer to coordinates in the plane). Of course, we are simply looking at the p evolution; the v evolution is taking place on the unit sphere. In some of the examples, there seems to be interesting regularity to the solution path; but at least one of the pictures seems to show rather chaotic behavior.

Consider Figures 5 and 6. The displacement function and initial position are the same; only the inclination (initial v) is different. for Figure 6, the v is nearly horizontal. The two trajectories (or more precisely, their projection onto the p coordinates) in both cases lie within the unit circle, but the second is somewhat striking in that the trajectories look like billiard paths (straight) and, at least from the graphic, it looks like the reflection angle is the appropriate one for Snell’s law to hold. Here is a simple heuristic argument as to why this should be the case.

First of all, it is worth looking at the simple displacement function $f(p_1, p_2) = -p_1$. In this case, the relevant differential equations are:

$$\begin{aligned} \frac{dp_1}{dt} &= p_1 v_1, \\ \frac{dp_2}{dt} &= p_1 v_2, \\ \frac{dv_1}{dt} &= v_3^2, \\ \frac{dv_2}{dt} &= 0, \\ \frac{dv_3}{dt} &= -v_3 v_1 \end{aligned}$$

The equations are simple enough so that they can be solved explicitly: assuming the third coordinate of the the initial vector v is positive, and that the initial position p has

negative horizontal component, then one can show that the resulting trajectories are of the form

$$(p_2 - A)^2 - B^2 p_1^2 = -C^2,$$

a hyperbola whose axis of symmetry is horizontal (and hence perpendicular to the line $f = -p_1 = 0$). (See Figure 7).

This easily extends to the general linear case: If $f(p_1, p_2) = ap_1 + bp_2$; and if we assume a starting point p with $f(p) \geq 0$ and initial vertical velocity component positive, then the associated solutions curves are hyperbolae whose axis of symmetry is parallel to $\nabla f = [a, b]$.

Now, consider an f with the following properties: f is regular at the points p where $f = 0$; that the regular curve Γ defined by $f(p) = 0$ is convex and bounded; and that the function is positive on the interior of the regular curve. Let's start off with a nearly horizontal initial pseudo-velocity vector $v_0 = (v_1, v_2, \epsilon)$, where ϵ is a small positive constant. If we consider the system Eqn (2), we see that v is changing extremely slowly (and in particular, the rate of change of the tangential part of v is of order ϵ^2), so for a period of time the direction of the velocity of p is nearly constant even if the speed is varying; hence the trajectory of p is nearly a straight line. However, as we approach a point γ of the boundary curve Γ , and $f(p)$ approaches zero, the dynamics mimics the behavior of the trajectories associated with the function g which is the linearization of f at γ ; the trajectories of g look nearly like straight lines which reflect as in Snell's law. Our informal discussion leads to the conclusion that *as the v vector becomes horizontal, trajectories of Eqn (3) approach the orbits of the billiard problem associated with the curve $f = 0$* . Of course, there is another method for obtaining billiard dynamics from a related smooth dynamical system: the Birkhoff construction of looking at geodesic flow on "pancake"-like surfaces, and letting the thickness of the surfaces go to zero (see [8]) We observe that the two constructions are quite different

7 Variational formulation

In this section, we work with flat templates. We describe how the thin film equations are related to a variational problem, which for certain examples simplifies the solution of the thin film equations. We then give two examples of thin films on flat templates, with displacement functions such that the associated thin film equations are integrable. We will discuss the first (and easier one) in some detail; we examine the second one only briefly.

7.1 Variational formulation

Define $N = n - 1$. The thin film equations for a flat template in R^{N+1} can be written:

$$\dot{v}_{N+1} = \sum_{k=1}^N v_k \frac{\partial f}{\partial q_k}; \quad \dot{v}_k = -v_{N+1} \frac{\partial f}{\partial q_k}, \quad \dot{q}_k = \frac{-f}{v_{N+1}} v_k, \quad k = 1 \dots N$$

Note that $\sum_{j=1}^{N+1} \dot{v}_j v_j = 0$, so the condition $\sum_{j=1}^{N+1} v_j^2 = c$ is preserved by the flow. Without loss of generality, we can assume $c = 1$.

If we define $D \equiv \sqrt{1 - \sum_{k=1}^N v_k^2}$, then we can rewrite our equations with v_{N+1} eliminated, obtaining the reduced form:

$$\dot{v}_k = -D \frac{\partial f}{\partial q_k}, \quad \dot{q}_k = -\frac{f}{D} v_k, \quad k = 1 \dots N$$

Now consider curves which lie in the hyperplane $v_{N+1} = 0$, with functional:

$$\mathcal{F} = \int F(q_1, \dots, q_n, \dot{q}_1, \dots, \dot{q}_N) dt, \quad F = \sqrt{\sum^N (\dot{q}_k)^2 + f^2(q_1, q_2, \dots, q_n)}$$

Of course, F is the Lagrangian. The procedure for computing the associated Hamiltonian and Hamilton's equations is routine ([9]) Define

$$p_k = \frac{\partial F}{\partial \dot{q}_k} = \frac{1}{D} \dot{q}_k,$$

which gives p_k in terms of \dot{q}_k . We need to solve the equations for \dot{q}_k in terms of p_k ; a bit of algebra leads to

$$\dot{q}_k = \frac{p_k f}{E}, \quad E = \sqrt{1 - \sum^N p_j^2};$$

one can check directly that these formulas work.

The Hamiltonian is $H = F - \sum^N \dot{q}_k p_k$, which translates into (now that we have \dot{q}_k in terms of p_k) $H = fE$. Then one computes Hamilton's equations

$$\dot{q}_k = \frac{\partial H}{\partial p_k}, \quad \dot{p}_k = -\frac{\partial H}{\partial q_k},$$

which for our problem become

$$\dot{q}_k = -\frac{f p_k}{E}, \quad \dot{p}_k = -\frac{\partial f}{\partial q_k} E$$

which are exactly the reduced thin film equations given above, with v_k replaced with p_k . Making this identification, we observe that $H = fE = f\sqrt{1 - \sum^N p_j^2} = f\sqrt{1 - \sum^N v_j^2} = f v_{N+1} = \langle v, N \rangle f$; thus we could have "guessed" the form of H .

7.2 The Spherical Displacement Function

Consider a flat template in the plane, with "spherical" displacement function $f(q_1, q_1) = \sqrt{1 - q_1^2 - q_2^2}$. By "spherical", we simply mean that when the "small" parameter ϵ is set equal to 1, the graph of f gives a (hemi-) sphere. Then, as discussed at the beginning of this section, the associated variational problem is to find critical points for the functional

$$\mathcal{F} = \int \sqrt{\dot{q}_1^2 + \dot{q}_2^2 + 1 - q_1^2 - q_2^2} dt$$

Given the symmetry of the problem, it is hardly surprising that we can solve the associated equations exactly; but on the other hand a complete analysis of the problem can be useful in understanding more complicated problems. It is useful to transform this into a functional on curves parameterized in polar coordinates $q_1 = r \cos(\theta)$, $q_2 = r \sin(\theta)$:

$$\mathcal{F}_{polar} = \int \sqrt{\dot{\theta}^2 r^2 + \dot{r}^2 + 1 - r^2} dt$$

The associated Euler-Lagrange equations are:

$$\ddot{r} = \frac{r(\dot{\theta}^2 r^2 - r^2 + 2\dot{r}^2 - \dot{\theta}^2 + 1)}{r^2 - 1}, \quad \ddot{\theta} = 2 \frac{\dot{r} \dot{\theta}}{r(r^2 - 1)}$$

A plot of an example solution curve, given by numerically solving these differential equations, is given in Figure 8. The initial conditions for this example are:

$$\left\{ r(0) = (1/2), \theta(0) = 0, \dot{r}(0) = 0, \dot{\theta}(0) = (3/7) \sqrt{21} \right\}$$

We now continue to find explicit solutions.

Observe that the second order equation for θ , is linear and easily solved in terms of r :

$$\theta(t) = D + C \int \frac{(r(t))^2 - 1}{(r(t))^2} dt$$

For the moment, we assume $D = 0$. We can substitute this formula for θ into the differential equation for r , to obtain

$$\ddot{r} = \frac{C^2 r^6 - 3C^2 r^4 - r^6 + 2\dot{r}^2 r^4 + 3C^2 r^2 + r^4 - C^2}{r^3(r^2 - 1)}$$

Of course, this is second order in r with an auxiliary parameter C . To solve this, we consider the ansatz

$$r = \sqrt{a + b(\operatorname{sn}(ct, k))^2}$$

and then see what the required relations are between the constants a, b, c, k required so that the ansatz does indeed give a solution. After some manipulation, one obtains a two parameter family of solutions of the form of the ansatz:

$$r = \sqrt{(\sin(w))^2 (\sin(v))^2 \left(\operatorname{sn} \left(\frac{t}{\cos(w) \sin(v)}, \sin(w) \right) \right)^2 + (\cos(v))^2}$$

corresponding to the C value

$$C = -\frac{\sqrt{-(\cos(w))^2 (\sin(v))^2 + 1} \cos(v)}{\cos(w) (\sin(v))^2}$$

The parameters v, w range between 0 and $\frac{\pi}{2}$.

With the explicit formula for r and C , we can go back to finding an explicit formula for θ . The formula given above for θ involves an antidifferentiation whose integrand is an elliptic function; fortunately, this is a doable integral, and we finally obtain

$$\begin{aligned} \theta(t) = & \left(\sqrt{-(\cos(w))^2 (\sin(v))^2 + 1} \right) \\ & \times \Pi \left(\operatorname{sn} \left(\frac{t}{\cos(w) \sin(v)}, \sin(w) \right), -\frac{(\sin(v))^2 (\sin(w))^2}{(\cos(v))^2}, \sin(w) \right) (\cos(v))^{-1} (\sin(v))^{-1} \\ & - \frac{\sqrt{-(\cos(w))^2 (\sin(v))^2 + 1} \cos(v) t}{\cos(w) (\sin(v))^2} \end{aligned}$$

where Π (with three arguments) is defined as the incomplete elliptic integral

$$\Pi(x, c, k) = \int_0^x \frac{dx}{(-cx^2 + 1) \sqrt{-x^2 + 1} \sqrt{-k^2 x^2 + 1}};$$

and Π with two arguments is the complete elliptic integral

$$\Pi(c, k) = \int_0^1 \frac{dx}{(-cx^2 + 1) \sqrt{-x^2 + 1} \sqrt{-k^2 x^2 + 1}}.$$

Since the Euler equations are second order in r, θ , one expects a four parameter family of solutions for the equations. As presented, we only have a two parameter family of solutions, which are distinguished by the fact that they satisfy the conditions $\dot{r}(0) = 0, \theta(0) = 0$. However, observe that our equations have two symmetries which we can exploit: the equations are invariant under $t \rightarrow t + c, \theta \rightarrow \theta + d$. These two extra degrees of freedom allow us to generate all solutions to the Euler equations.

Given these explicit formula for r and θ , we can read off interesting geometric information about the solutions. Consider the formula given above for r . Since $\text{sn}(x, k)$ ranges between 0 and 1 as x ranges between 0 and $K(k)$ (the complete elliptic integral of the first kind), we see that r ranges between $r_{\min} = \cos(v)$ and $r_{\max} = \sqrt{(\sin(w))^2 (\sin(v))^2 + (\cos(v))^2}$. In fact, $r(0) = r_{\min}$ and $\dot{r}(0) = 0$. Also, $\theta(0) = 0$ and $\dot{\theta}(0) = \frac{\sqrt{-(\cos(w))^2 (\sin(v))^2 + 1}}{\cos(v) \cos(w)}$. This allows us, by appropriate choice of v, w to construct solutions with r_{\min}, r_{\max} as desired. For example, for the choice $r_{\min} = 1/2, r_{\max} = 3/4$, one readily checks that $v = \frac{\pi}{3}, w = \arcsin((1/6)\sqrt{15})$; and for this choice of the pair v, w , we have $\dot{\theta}(0) = (3/7)\sqrt{21}$, which gives us exactly the initial conditions for our numerically computed example. We now know that our solution curve is "trapped" between the two circles of radii 1/2 and 3/4 respectively. In Figure 9 the same solution curve, these two circles, and the circle of radius 1 are plotted simultaneously. The initial conditions were chosen so that the inner and outer radii have simple values.

Figure 9 suggests that there is a periodic orbit nearby with five "lobes". Indeed, resorting again to the explicit formula for r and θ we can find closed solutions (periodic orbits) for our equations.

First, let's consider the periodicity of r . Since $\text{sn}(x, k)^2$ is $2K(k)$ -periodic, then we can see that r has period $2K(\sin(w)) \cos(w) \sin(v)$. Over this interval, one checks that θ is changed by an increment of

$$\Delta = -2 \sqrt{-(\cos(w))^2 (\sin(v))^2 + 1} \\ \times \left(K(\sin(w)) (\cos(v))^2 - \Pi \left(-\frac{(\sin(w))^2 (\sin(v))^2}{(\cos(v))^2}, \sin(w) \right) \right) (\cos(v))^{-1} (\sin(v))^{-1}$$

Thus, to obtain a closed curve, we need $\frac{\Delta}{2\pi}$ to be rational. Suppose, for example, we wish to find a five-lobe solution to our equations; we need $\frac{\Delta}{2\pi} = \frac{2}{5}$. We look for a solution close to the non-periodic solution plotted in Figure 9; so we again set $v = \frac{\pi}{3}$, thus setting $r_{\min} = 1/2$. Then, we are asking for a solution to

$$\frac{4\pi}{5} = -2/3 \sqrt{-3/4 (\cos(w))^2 + 1} (\sqrt{3}K(\sin(w))) \\ + 8/3 (\sqrt{-3/4 (\cos(w))^2 + 1}) \sqrt{3} \Pi(-3 (\sin(w))^2, \sin(w))$$

and one obtains numerically $w = 0.6281734812$. Note that this not only gives closure; having this value allows us to compute $r_{\max} = 0.7134529902$, compared to $r_{\max} = .75$ for our previous example.

We now look at this example directly from the variational point of view (rather than looking at the Euler equations directly). In rectangular coordinates, the integrand of the functional (the Lagrangian) $F = \sqrt{\dot{q}_1^2 + \dot{q}_2^2 + 1 - q_1^2 - q_2^2}$. This has two symmetries that we exploit using Noether's theorem. The first is the independence of the Lagrangian with respect to the variable of integration t ; the second is the invariance with respect to rotation. The first leads to the "constant of motion" $H = F - \dot{q}_1 F_{\dot{q}_1} - \dot{q}_2 F_{\dot{q}_2}$, and the second leads to the constant of motion $L = F_{\dot{q}_1} q_2 - F_{\dot{q}_2} q_1$, or equivalently

$$H = -\frac{q_1^2 + q_2^2 - 1}{\sqrt{\dot{q}_1^2 + \dot{q}_2^2 - q_1^2 - q_2^2 + 1}}, \quad L = \frac{\dot{q}_1 q_2 - \dot{q}_2 q_1}{\sqrt{\dot{q}_1^2 + \dot{q}_2^2 - q_1^2 - q_2^2 + 1}}$$

Of course, these can both be converted into polar coordinates;

$$H = -\frac{r^2 - 1}{\sqrt{r^2 \dot{\theta}^2 - r^2 + \dot{r}^2 + 1}}, \quad L = -\frac{r^2 \dot{\theta}}{\sqrt{\dot{\theta}^2 r^2 + \dot{r}^2 - r^2 + 1}}$$

We now give an informal argument showing that r_{min} and r_{max} can be expressed in terms of these conserved quantities H and L . Suppose we are at a point where $\dot{r} = 0$ (for example, when $r = r_{min}$ or $r = r_{max}$). Then the above formulas simplify:

$$H = -\frac{r^2 - 1}{\sqrt{\dot{\theta}^2 r^2 - r^2 + 1}}, \quad L = -\frac{r^2 \dot{\theta}}{\sqrt{\dot{\theta}^2 r^2 - r^2 + 1}}$$

So if we are at a point where $\dot{r} = 0$, then we can solve for the values of r and $\dot{\theta}$ in terms of H and L ; and in particular we obtain the following formulas for r , which we give temporary names U and V :

$$U = 1/2 \sqrt{2 - 2H^2 + 2L^2 - 2\sqrt{H^4 - 2H^2L^2 + L^4 - 2H^2 - 2L^2 + 1}},$$

$$V = 1/2 \sqrt{2 - 2H^2 + 2L^2 + 2\sqrt{H^4 - 2H^2L^2 + L^4 - 2H^2 - 2L^2 + 1}}$$

From the formulas, it is clear that $V > U$. As we move along the curve, both U and V are constant; and at a point where $r = r_{min}$ or $r = r_{max}$, one of these two functions gives the r value at that point. Henceforth, we denote U by r_{min} and V by r_{max} .

Obviously, the formulas above are somewhat awkward. One can check that the inverse formulas are much cleaner; in fact:

$$r_{min} r_{max} = L, \quad r_{min}^2 + r_{max}^2 = L^2 + 1 - H^2$$

7.3 The Ellipsoid

We consider the ellipsoidal displacement function $f = \sqrt{1 - \sum_{i=1}^N \frac{x_i^2}{a_i^2}}$. From Figures 11 and 12, we see a regularity of orbits for the associate TFE with $N = 2$ which suggests the problem is integrable. As a step towards substantiating this, we record constants of motion associated with this problem: define $x_{N+1} = 0, a_{N+1} = 0$, then the functions

$$I_k = v_k^2 + \sum_{j=1, j \neq k}^N \frac{(-x_k v_j + v_k x_j)^2}{-a_j^2 + a_k^2}, \quad k = 1 \dots N + 1$$

are conserved quantities (“integrals of motion”). Although this list includes $N + 1$ conserved quantities, one checks that $\sum_{k=1}^{N+1} I_k = \sum_{k=1}^{N+1} v_k^2$; and this last sum is a conserved quantity for any thin film equation (a Casimir for our setup). One checks that the Poisson bracket $\{I_j, I_k\} = 0$, that is, the functions are in involution. It is also possible to obtain these constants of motion by considering the first integrals for geodesic flow on the ellipsoid ([10]), and then taking the limit as the thickness of the ellipsoid goes to zero.

8 “Nearly thin” double mirror systems and TFE’s: a “numerical analysis” perspective

Suppose we have a surface M , a displacement function f (which we assume to be strictly positive) and the nearby surface $M_\epsilon = \{p + \epsilon f(p)N(p), p \in M_0\}$, where ϵ is small, fixed, and positive. Suppose we have a point p_0 on M , and an initial unit pseudo-velocity vector v_0 . We can then do a “double reflection” as in Figure 1, obtaining a new point and pseudo-velocity p_1 and v_1 . Alternatively, we can solve the differential equation system $(\dot{v}, \dot{p}) = \chi(v, p)$ with initial conditions $v(0) = v_0, p(0) = p_0$ and ask for the values of $v(\epsilon)$ and $p(\epsilon)$, and ask how close these values are to v_1 and p_1 . One can think of the mapping $(v_0, p_0) \rightarrow (v_1, p_1)$ as a (not very efficient!) way of obtaining a discrete approximation to v_1 and p_1 , just as one does in numerical analysis. What sort of estimates can one make?

Such a result may be useful in a subsequent paper (see concluding remarks), but here we will just sketch the results associated to a very elementary example, which we believe exhibits the behavior of the more general problem. The full details will have to appear in a sequel.

We work in two dimensions, and M is the straight line (one-dimensional flat template!) $p_2 = 0$. Assume $p_0 = 0$, $v(0)$ not horizontal and $f(p) = a + bp + cp^2$. Then one can do the following two calculations (greatly facilitated by symbolic calculation): (i) Calculate, to third order in ϵ , the reflected point p_1 and v_1 ; and (ii) Calculate a series expansion in ϵ , up to third order, for the solution $v(\epsilon), p(\epsilon)$ of the system $(\dot{v}, \dot{p}) = \chi(v, p)$ with $v(0) = v_0, p(0) = p_0$. Comparing these two expansions, one sees that the difference is $O(\epsilon^3)$. Typical arguments in numerical analysis ([11]) in numerical analysis show that, if the error associated with this single time-step is $O(\epsilon^3)$, then the difference between (v_N, p_N) and $(v(N\epsilon), p(N\epsilon))$ is $O(\epsilon^2)$.

9 Bracket Structure

Obviously, the set of all functions of the form $H_f = \langle v, N \rangle f$ (as before, $f : M \rightarrow R$) forms a vector subspace of the set of all functions on G_2 . We ask how they behave with respect to the Poisson bracket associated with the symplectic form on G_2 . We record a couple of relevant formulas. First, some notation. As before, we have $H_f(v, p) = \langle v, N(p) \rangle f(p)$. Let \mathbf{w} be a vector field on M , then $H_{\mathbf{w}}(v, p) = \langle v, \mathbf{w} \rangle$. We have:

$$\begin{aligned} \{H_f, H_g\} &= H_{f\nabla g - g\nabla f} \\ \{H_{\mathbf{w}_1}, H_{\mathbf{w}_2}\} &= H_{[\mathbf{w}_1, \mathbf{w}_2]} \end{aligned}$$

The proof of these formulas in the simple case where M is the flat hyperplane $x_n = 0$, in standard Euclidean coordinates, is elementary. We then observe that, in any coordinate representation, all of the quantities involved are first order, and invariant under translations and rotations; hence can be reduced to the simple case just discussed. Note that the second formula shows an isomorphism between the Lie algebra of vector fields along M , and their

associated Hamiltonians. Of course, if P is a manifold and T^*P is its cotangent bundle, then any vector field on P lifts (locally) to a hamiltonian vector field on T^*P . Since G_2 is (by definition) symplectomorphic to T^*S^n , it is not surprising that a similar statement holds in our situation; it is nice that the form of the equations works out so cleanly.

It would be interesting to understand the full Lie algebra generated by the Hamiltonians H_f .

10 Concluding Remarks and Related questions

Of course, ray optics is derived from Maxwell's equations by taking the limit as frequency λ becomes large. In this paper we let the thickness ϵ of the double mirror system (thin film) go to zero *after* letting λ approach infinity. Clearly, it would be more realistic to have some coupling between λ and ϵ so that they go to infinity and zero respectively at the same time. This is an important aspect of the problem which we wish to pursue in the future.

In [12], Pierone has a result which, translated into the language of our paper, says that for a positive displacement function f and for ϵ small (but not zero), the billiard problem is transitive on configuration space: given two points p_0, p_1 on M , there is a starting direction vector v_0 such that by going out along v_0 starting from p_0 , one lands at p_1 after sufficiently many reflections. We are hoping that the considerations of this paper will allow for a simpler proof of Pierone's result, by approximating the (discrete) billiard trajectories by the (continuous) trajectories of χ_f . Hopefully, the considerations of Section 8 will prove useful here.

The variational problem associated with geodesics on a manifold is of course $\mathcal{L} = \int \sqrt{\Sigma g_{ij} \dot{\gamma}_i \dot{\gamma}_j} ds$. As suggested by Section 7, one could instead consider the generalization $\mathcal{F} = \int \sqrt{f^2 + \Sigma g_{ij} \dot{\gamma}_i \dot{\gamma}_j} ds$, associated with a displacement function f . What properties of geodesic flow are preserved, or can be preserved, by this perturbation of \mathcal{L} ? For example, if the geodesic equations are integrable, are there f for which the Euler-Langrange equations are integrable? In a subsequent paper, we discuss such questions in the context of thin film equations associated to conics.

11 Acknowledgements

This paper would not exist without the catalyst of various communications with Sergei Tabachnikov, both in person and via email, to whom I owe great thanks. The ICERM Conference on Integrability in June 2015 gave me the opportunity to discuss these ideas with the many visitors there, and I want to thank the organizers of the conference as well as ICERM itself for making it all pleasant and possible. Various colleagues have discussed some of these ideas with me at length; in particular I want to thank Joel Langer of Case Western Reserve and Doug Wright of Drexel for their attention and advice.

References

- [1] O. S. Heavens. *Optical Properties of Thin Solid Films*. Courier Corporation.
- [2] H. Angus MacLeod. *Thin-Film Optical Filters, Fourth Edition*. CRC Press.
- [3] V. Russo G C Righini. Geodesic lenses for guided optical waves. 12(7):1477–81.

- [4] R. Ulrich and R. J. Martin. Geometrical optics in thin film light guides (applied optics). 10(9):2077.
- [5] Ralph Abraham and Jerrold E. Marsden. *Foundations of Mechanics*. American Mathematical Soc.
- [6] Charles-Michel Marle. A direct proof of malus' theorem using the symplectic structure of the set of oriented straight lines (arxiv preprint).
- [7] Victor Guillemin and Shlomo Sternberg. *Geometric Asymptotics*. American Mathematical Soc.
- [8] Serge Tabachnikov. Projectively equivalent metrics, exact transverse line fields and the geodesic flow on the ellipsoid (comm. math. helv.). 74(2):306–321.
- [9] Izrail Moiseevitch Gelfand, Serge Vasilevich Fomin, and Richard A. Silverman. *Calculus of Variations*. Courier Corporation.
- [10] Serge Tabachnikov. *Geometry and billiards*, volume 30. Amer Mathematical Society.
- [11] Germund Dahlquist and Ake Bjorck. *Numerical Methods*. Courier Corporation.
- [12] Roberto Peirone. Billiards in tubular neighborhoods of manifolds of codimension 1 (comm. math. phys.). 207(1):67–80.

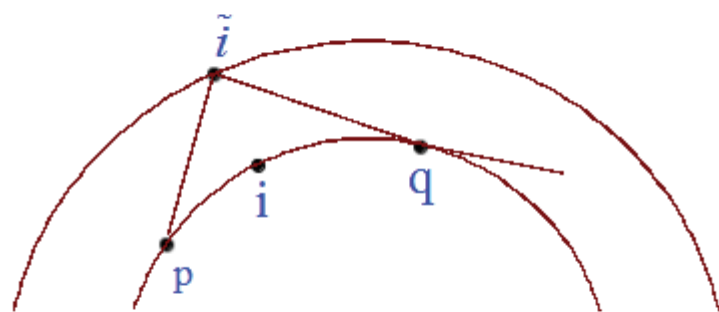


Figure 1

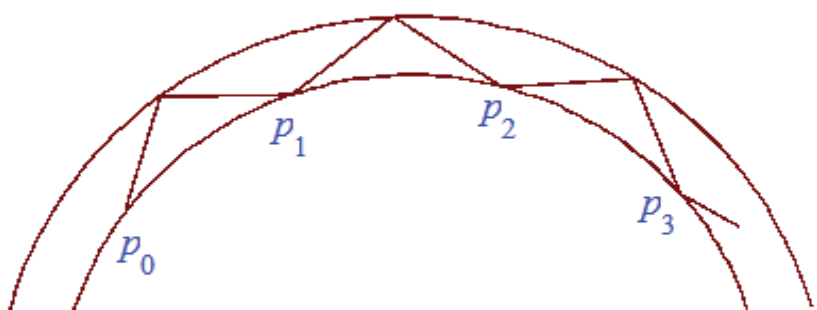


Figure 2

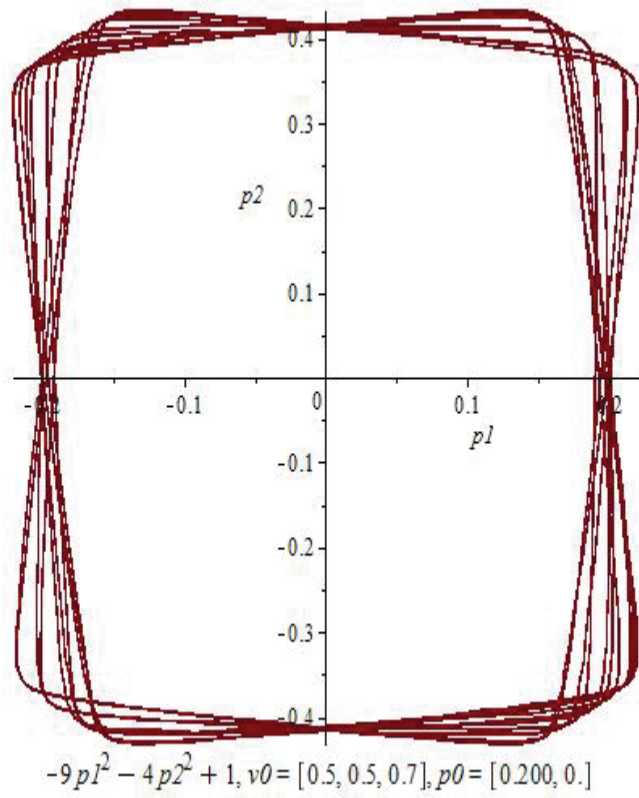


Figure 3

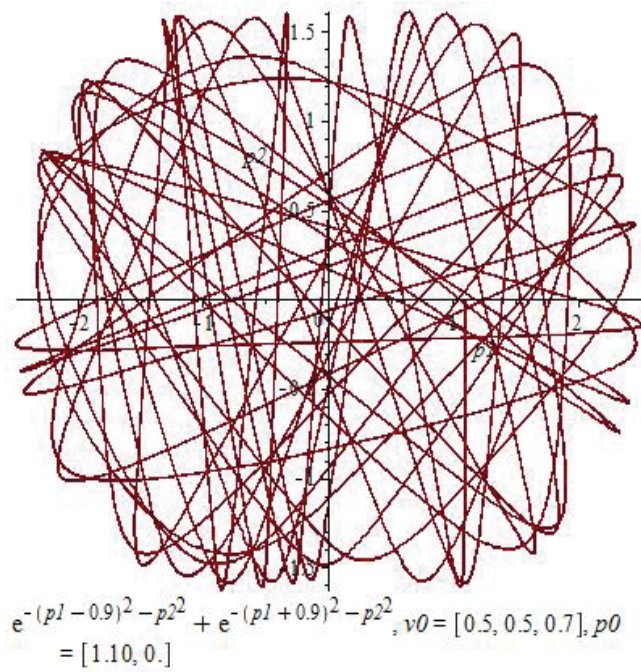
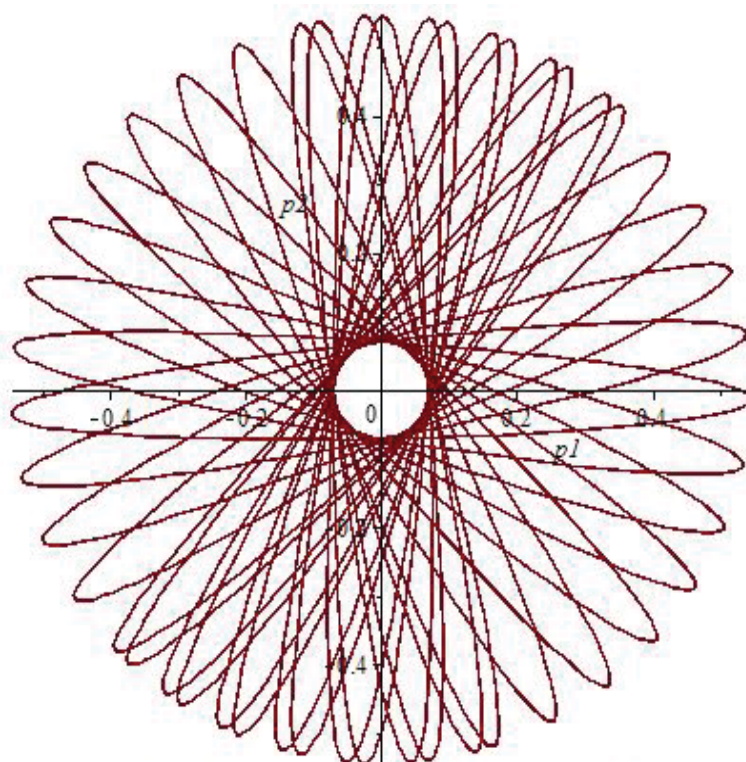
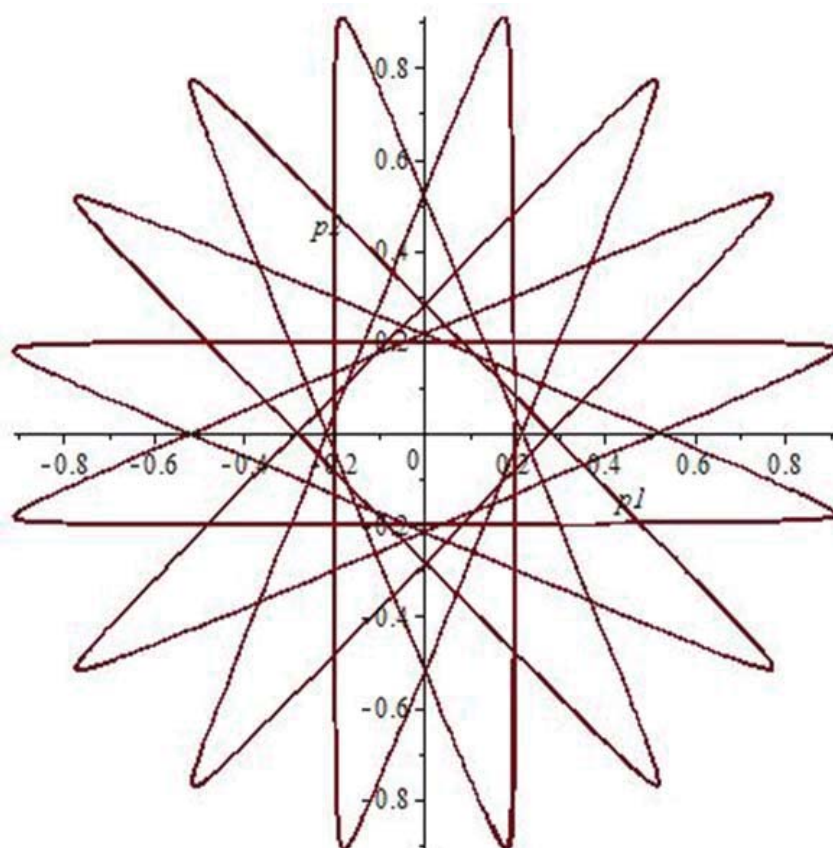


Figure 4



$$-p_1^2 - p_2^2 + 1, v_0 = [0.5, 0.5, 0.7], p_0 = [0.1, 0.]$$

Figure 5



$$-p_1^2 - p_2^2 + 1, v_0 = [0.5, 0.5, .01], p_0 = [0.1, 0]$$

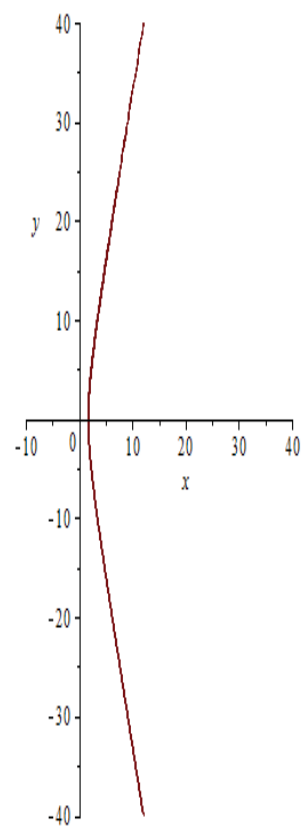
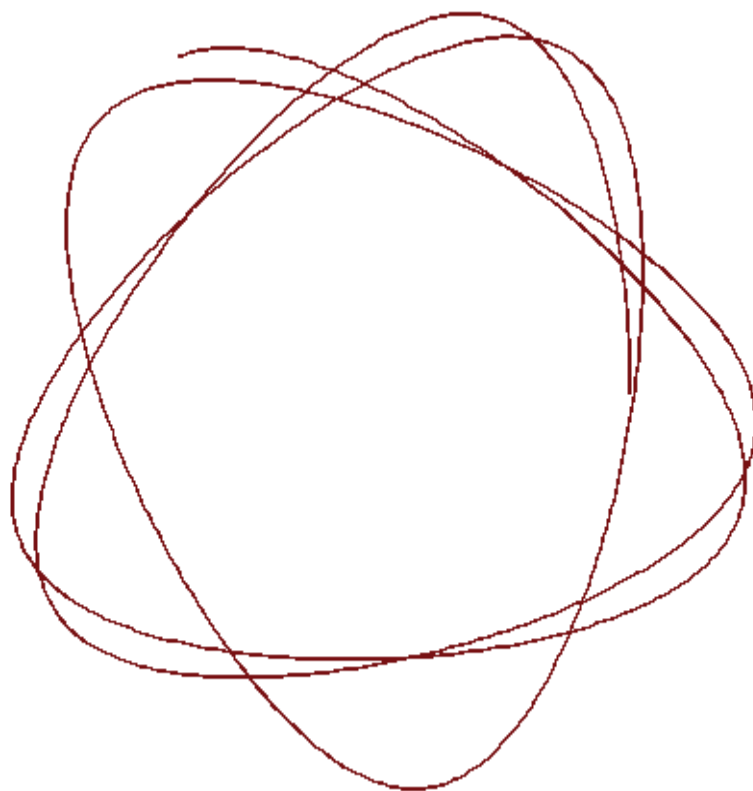


Figure 7



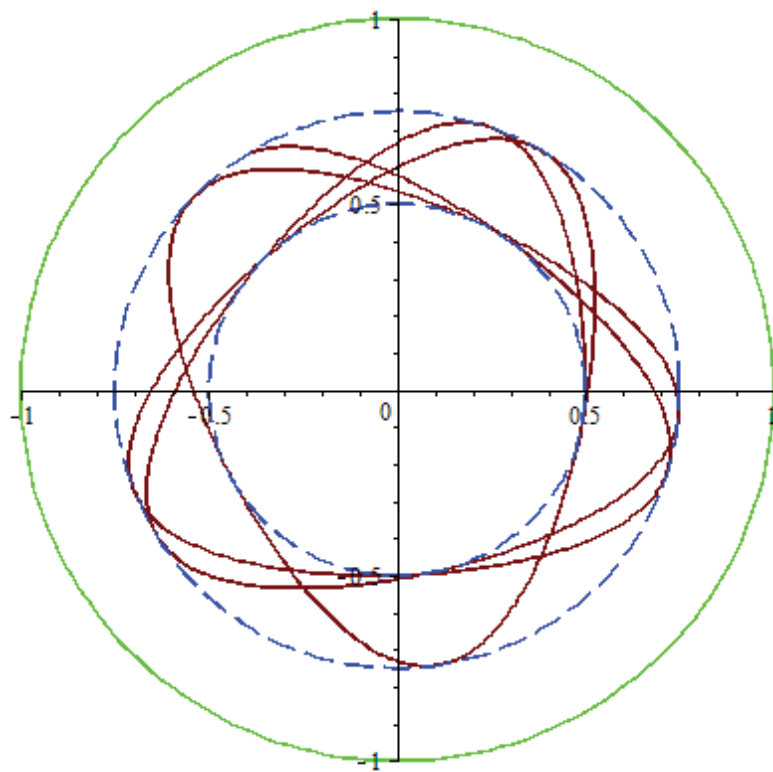
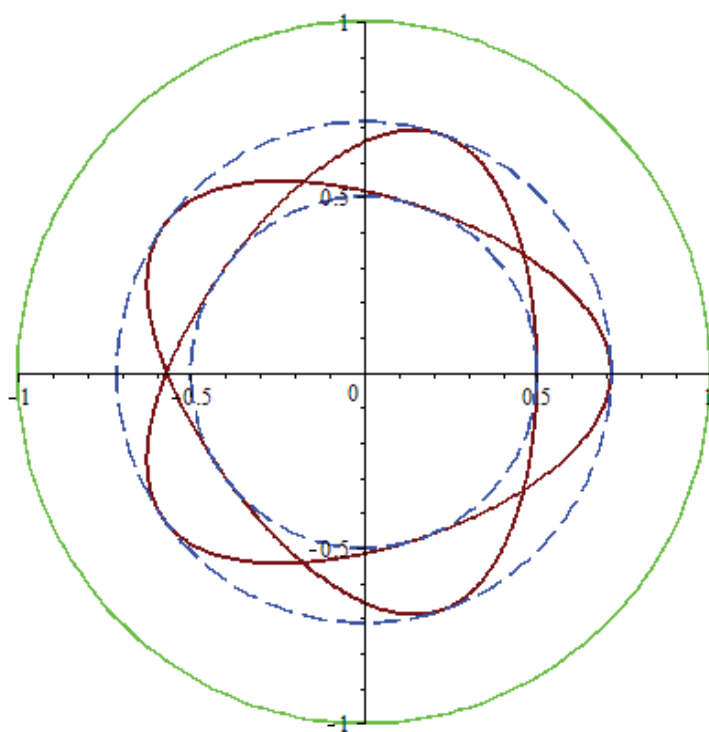


Figure 9



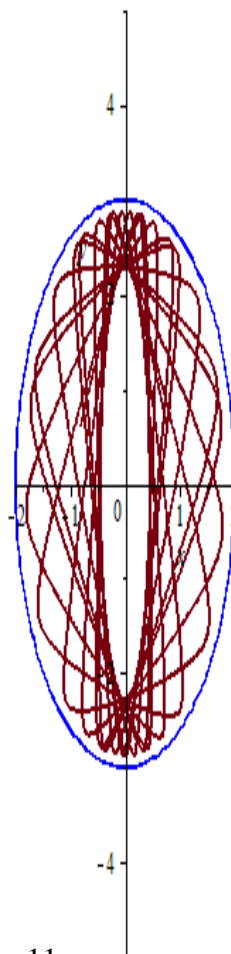


Figure 11

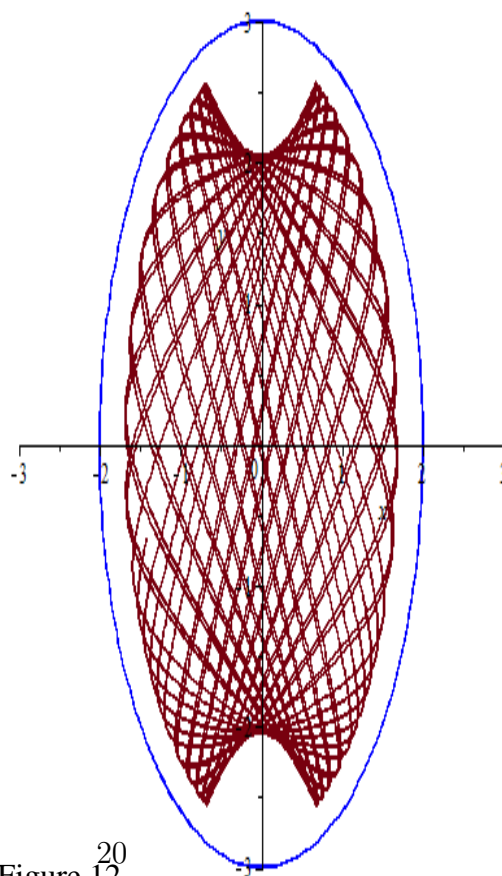


Figure 12